Spatial and temporal variability in organic carbon burial during global positive carbon isotope excursions: New insight from high resolution $\delta^{13}C_{carb}$ stratigraphy from the type area of the Niagaran (Silurian) Provincial Series

Bradley D. Cramer[1], Matthew R. Saltzman[1], Mark A. Kleffner[2]
[1]*The Ohio State University, 125 S. Oval Mall, Columbus, OH 43210*
[2]*The Ohio State University-Lima, Science Building, Lima, OH 45804*
e-mail: cramer.70@osu.edu

ABSTRACT: Ninety-four carbonate samples were analyzed for carbon isotope ($\delta^{13}C_{carb}$) stratigraphy from the Niagara River Power Project S-1 core, Lewiston, New York. Samples were taken from Clinton and Lockport Group rocks in the type area of the Niagaran Provincial Series in order to constrain more precisely the age and correlation of middle Silurian strata of the Appalachian Basin. The well known, Ireviken (Sheinwoodian), positive carbon isotope excursion is present in the sampled section, and indicates that the Irondequoit, Rochester, Decew, Gasport, and Goat Island Formations are all Sheinwoodian in age. This fact has implications for both stratigraphic correlation of Silurian strata throughout North America as well as the interpretation of the stratigraphic record with respect to positive carbon isotope excursions. Here, we discuss the Appalachian Basin sequence in the context of an oceanographic model that links changes in global oceanography with alternations between cold and warm climate states.

INTRODUCTION

The presence of at least four major (>+4‰) positive carbon isotope excursions (Samtleben et al. 1996; Bickert et al. 1997; Azmy et al. 1998; Saltzman 2001; 2002a; Calner et al. 2004) during the Silurian, which was only ~23myr in duration (Melchin et al., 2004), provides a unique opportunity for the use of carbon isotope stratigraphy as a powerful correlation tool. Unfortunately, Paleozoic carbon isotope stratigraphy is often performed at too low resolution, with individual excursions only being recognized by a handful of samples. Our investigation provides more than 60 samples within the Ireviken Excursion allowing for detailed correlation with sections globally.

Models of transient positive carbon isotope excursions (e.g. Arthur et al. 1987; Kump and Arthur 1999) frequently concentrate on the burial and sequestration of isotopically light carbon (^{12}C), in the form of organic matter, in organic-rich deposits. The fact that in the modern ocean, the majority of organic carbon burial takes place on the continental shelf and slope (Berner and Canfield 1989), has been applied to the epicontinental seas of the Paleozoic to conclude that major positive carbon isotope excursions should have been the result of intense organic carbon burial in epeiric sea settings. Combined with the fact that there is often a close stratigraphic association between epicontinental black shales and positive carbon isotope excursions, a causal relationship between individual epicontinental black shale deposits and individual positive carbon isotope excursions is often assigned (e.g. Joachimski and Buggisch, 1993; Brand et al., 2004). In contrast to this prediction, a high burial fraction of organic carbon in shallow marine settings is inconsistent with the prolific reef building and expansion of carbonate platforms that coincide with Silurian $\delta^{13}C$ excursions (Bickert et al. 1997; Brunton et al. 1998; Calner et al. 2004).

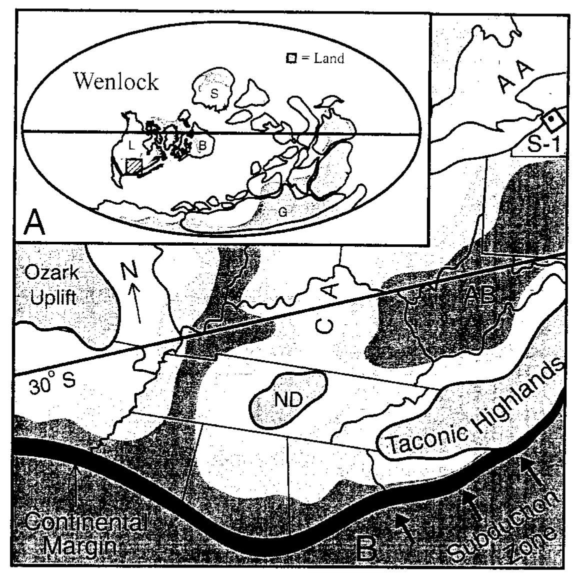

TEXT-FIGURE 1
Figure modified from Cramer and Saltzman (2005). Panel A: Wenlock paleogeography (after Woodcock 2000; Cocks 2001; and Johnson et al. 2001). Grey areas denote land. Capital letters refer to major emergent landmasses: (L) Laurentia; (B) Baltica; (S) Siberia; (G) Gondwana. Diagonally hatched box indicates area shown in panel B.Panel B: Paleogeographic and paleobathymetric reconstruction of the mid-continent of North America (compiled from Horvath 1969; Berry and Boucot 1970; Shaver 1996; and Brett 1999). Darker shaded areas of basins represent deeper water. Relative size and emergence of the Ozark uplift is speculative. Abbreviations: (AA) Algonquin Arch; (CA) Cincinnati Arch; (AB) Appalachian Basin; (ND) Nashville Dome. Black dot in upper-right corner indicates location of the Niagara River Power Project S-1 Core (S-1), Lewiston, New York. The white box around the study area represents the area depicted in text-figure 6.

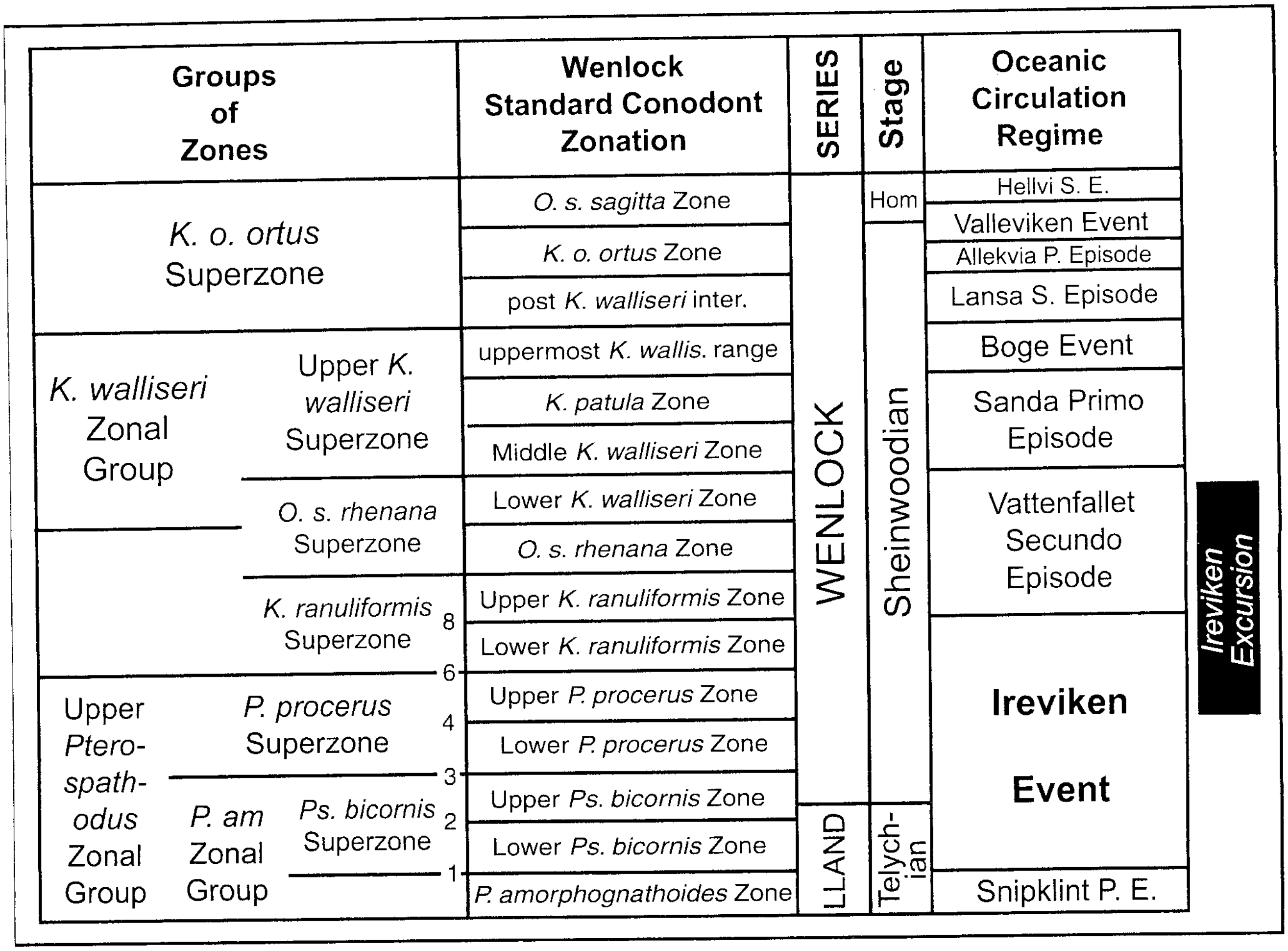

TEXT-FIGURE 2
Telychian through Homerian standard conodont zonation and groups of zones from Jeppsson (1997a). Oceanic regimes after Jeppsson (1993; et al. 1995). Duration of Ireviken Excursion from Calner et al. (2004). Illustrated length of zones is not intended to represent time.

This issue can be resolved however if elevated organic carbon burial took place in deeper water away from the shelf.

The Ireviken Excursion has been well documented in relatively shallow water settings throughout Baltica and Laurentia (Samtleben et al. 1996; Bickert et al. 1997; Kaljo et al. 1997; Saltzman 2001; Munnecke et al. 2003; Cramer and Saltzman 2005). This investigation allows for the first time a precise correlation of Appalachian Basin stratigraphy with respect to the Ireviken Excursion. We discuss the Appalachian Basin sequence in the context of an oceanographic model developed to account for Silurian climate change and suggest that the changes in global oceanography responsible for the Ireviken Excursion are illustrated in the Appalachian Basin.

GEOLOGICAL BACKGROUND

Geological Setting

Middle Silurian strata of western New York were among the first to be studied intensively in the United States, with the Rochester Shale being one of the first formally named stratigraphic units in North America (Hall 1839). The most recent formal revision of New York Silurian strata (Brett et al. 1995) indicates that the Niagaran Provincial Series contains strata from the Ordovician-Silurian boundary into the Ludlow, and is divided into three groups: stratigraphically from oldest to youngest, the Medina, Clinton, and Lockport Groups. Here, we sampled the upper Clinton and most of the Lockport Groups, with samples taken from the Williamson, Rockway, Irondequoit, Rochester, Decew, Gasport, Goat Island, and Eramosa Formations.

For this investigation, we sampled the Niagara River Power Project S-1 core, which was drilled on the site of what is now the Robert Moses Power Plant in Lewiston, New York. The core is available for future study through the New York State Museum in Rochester, NY. The precise locality of the core within New York was given as, Latitude: 43.14139°N, Longitude: 79.02639°W.

The study area (text-fig. 1) was located in the north-west corner of the Appalachian Basin on the distal edge of the southeast-facing limb of the Algonquin Arch (Ettensohn 1994; Goodman and Brett 1994; Ettensohn and Brett 1998; Brett, 1999). Western New York was located at 15°-30° S (Van der Voo 1988; Witzke and Scotese 1990; Woodcock 2000; Smethurst and McEnroe 2003) within the southern sub-tropical high pressure zone (Parrish 1982; et al. 1983; Baarli 1998). The structural axis of the Appalachian Basin had migrated back to the vicinity of Rochester, NY (~100 km east of the study area) by upper

Clinton times after predominantly eastward migration during the Llandovery (Goodman and Brett 1994).

Biostratigraphic Correlation of the Ireviken Excursion

The Sheinwoodian (Ireviken) positive carbon isotope excursion is an excellent stratigraphic marker for the Llandovery-Wenlock boundary and is present in the New York sequence. According to correlation between the GSSP (Global Stratotype Section and Point) for the Llandovery-Wenlock boundary at Leasows, UK, and the intensively studied sections of the Swedish island of Gotland, the Ireviken Excursion began immediately above the Llandovery-Wenlock boundary (Mabillard and Aldridge 1985; Jeppsson 1997a; Munnecke et al. 2003). A major biotic crisis, known as the Ireviken Event (Jeppsson 1983; 1987; 1997b) spanned the Llandovery-Wenlock boundary, severely affecting conodonts, graptolites, trilobites, and many other marine organisms (Mabillard and Aldridge 1985; Chatterton et al. 1990; Jeppsson 1990; 1997a; 1997b; Melchin 1994; Eriksson and Hagenfeldt 1997; Berry 1998; Mikulic and Kluessendorf 1999). The Ireviken Excursion began during this faunal turnover (text-fig. 2) and lasted much of the Sheinwoodian (Calner et al. 2004).

The onset of the Ireviken Excursion (onset of maximum rate of positive change) is precisely located at Datum 4 of the Ireviken Event (Munnecke et al. 2003), which marks the boundary between the Lower and Upper *Pterospathodus procerus* conodont Zones (Jeppsson 1997a). The extremely high resolution biostratigraphy of Gotland, which serves as the global standard for Wenlock conodont biostratigraphy is difficult to match elsewhere. In regions where the level of biostratigraphic detail is low, the onset of the Ireviken Excursion often appears near the last occurrence of the cosmopolitan conodont *Pterospathodus amorphognathoides* (Saltzman 2001; Cramer and Saltzman 2005). The Ireviken Excursion ended within the Lower *Kockelella walliseri* Zone (Calner et al. 2004).

METHODS AND RESULTS

Methods

High-resolution carbon isotope stratigraphy is only possible when micrite is the sampling medium. The use of brachiopods for carbon isotope stratigraphy, commonly assumed to be the most reliable material for chemostratigraphic investigation (e.g. Mii et al. 1999), restricts sampling to intervals or sections where brachiopods are available. Carbonate powders containing an admixture of select carbonate grains (i.e. crinoids, brachiopods, etc.) and primary marine micrite have been repeatedly demonstrated to faithfully record the original isotopic signature of Paleozoic marine waters (e.g. Saltzman 2005) and are available at any resolution in all carbonate sequences. Silurian micrites have been shown to preserve primary marine isotopic signatures (Saltzman 2001; Cramer and Saltzman 2005), while brachiopods and bulk rock samples from the same formation have been shown to produce nearly identical results (compare Munnecke et al. 1997 with Bickert et al. 1997). The reliability of micrite and fine grained carbonates for carbon isotope stratigraphy has been demonstrated in every system of the Paleozoic (Cambrian: Ripperdan et al. 1992; Saltzman et al. 1998; 2000, Ordovician: Finney et al. 1999; Kump et al. 1999, Devonian: Joachimski and Buggisch 1993; Wang et al. 1996, and Carboniferous: Saltzman 2002b).

The $\delta^{13}C$ signal in limestone is much more robust than $\delta^{18}O$ due to the substantially smaller amount of carbon in groundwater than the limestone through which it permeates. Several authors have demonstrated that late-stage post-depositional diagenesis of marine carbonate does not usually result in the resetting of $\delta^{13}C$ values (Magaritz 1983; Banner and Hanson 1990). Likewise, dolomitization has been shown to have a negligible effect on carbon isotope trends (Glumac and Walker 1998).

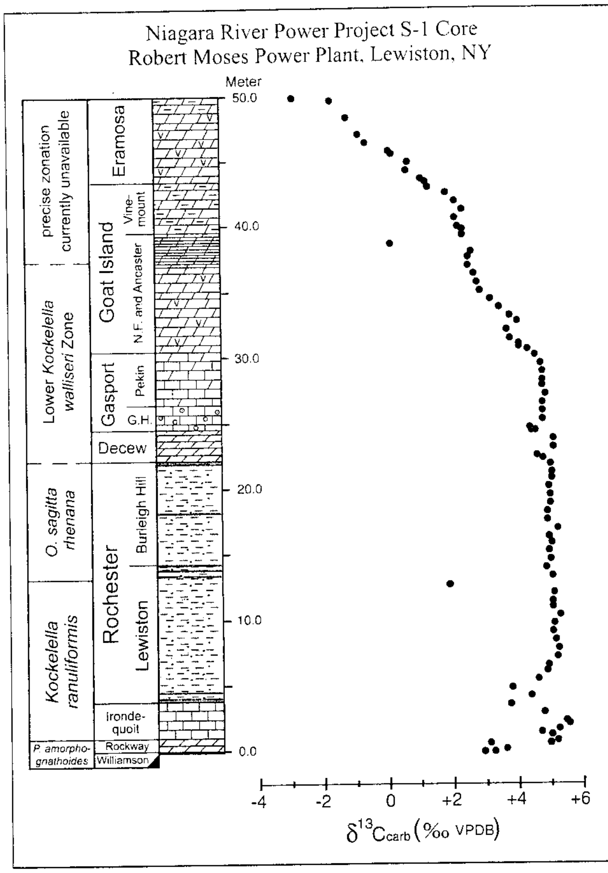

TEXT-FIGURE 3
Stable carbon isotope data from the Niagara River Power Project S-1 core. Conodont data from Kleffner (1991), Jeppsson (1997a), and unpublished data of MK. Meters to the right of the stratigraphic column represent meters above or below the Williamson-Rockway contact. Note the onset of the Ireviken Excursion near the Rockway-Irondequoit contact, and that the Rochester Shale is coincident with the peak values during the middle of the Ireviken Excursion. Carbon isotope values return to baseline (+2.5‰) in the Goat Island Formation marking the end of the Ireviken Excursion, therefore at least the Irondequoit, Rochester, Decew, Gasport, and Goat Island Formations are all Sheinwoodian in age.

Analyzed samples were drilled from the S-1 core with every effort made to sample only micrite, but some intervals were too coarse grained (e.g. crinoids and brachiopods) to guarantee that no carbonate grains were sampled. Samples were analyzed at the Stable Isotope Laboratory at the University of Saskatchewan. Carbonate powders were roasted in a vacuum oven at 200° C for 1 hour to remove water and volatile organic contaminants that may confound stable isotope values of carbonate. Stable isotope values were obtained using a Finnigan Kiel-III carbonate preparation device directly coupled to the dual inlet of a Finnigan MAT 253 isotope ratio mass spectrometer. 10-50 micrograms of carbonate was reacted at 70°C with 3-5 drops of an-

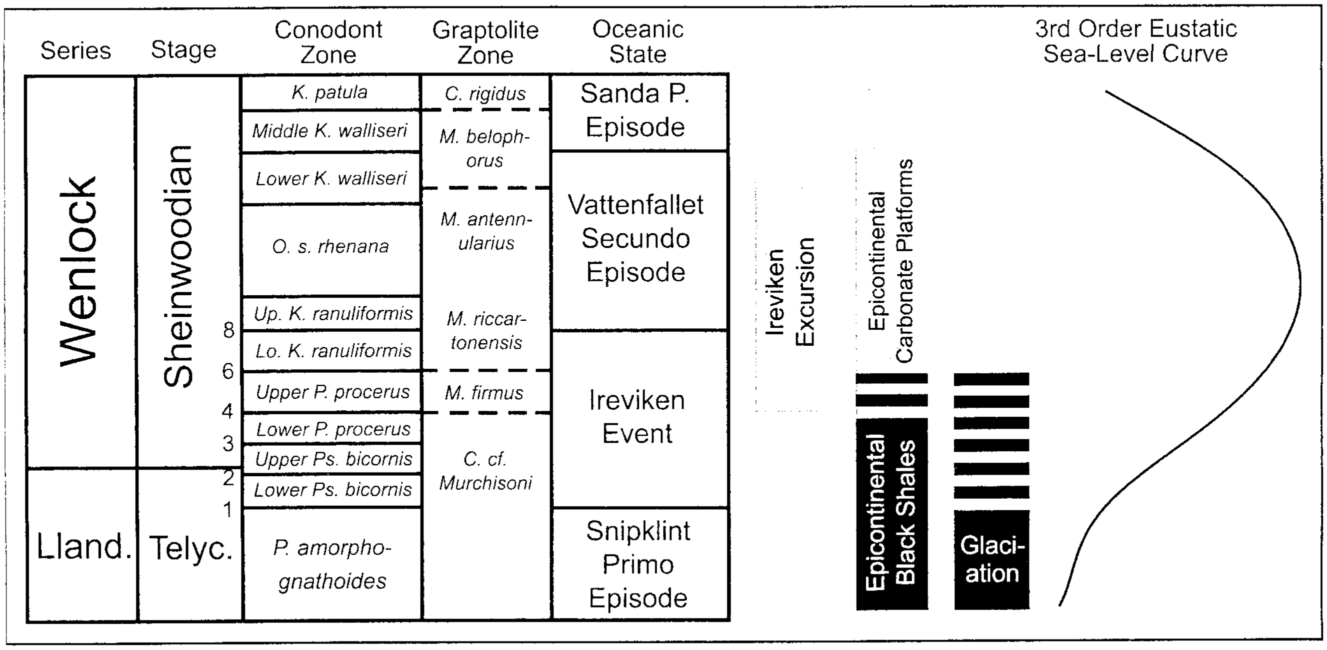

TEXT-FIGURE 4
Timing of epicontinental stratigraphy, glaciation, and eustatic sea-level change with respect to the Ireviken Excursion. Figure is not scaled to time. Biostratigraphy from Calner et al. (2004). The third-order sea level curve is from Cramer and Saltzman (2005). Note that the Williamson Shale was deposited during the widespread epicontinental organic burial interval of the latest Llandovery while the Rochester Shale was deposited during an interval dominated by carbonate production in low-mid latitude epeiric seas. The higher order sea-level cyclicity shown by the sequence boundaries within the sampled interval can be well correlated globally and clearly had little to no impact of carbon isotope values. It is the higher order (3^{rd}?) eustatic sea-level changes that the excursion mirrors.

hydrous phosphoric acid for 180-300 seconds. Isotope ratios were corrected for acid fractionation and ^{17}O contribution and are reported in per mil notation relative to the V-PDB standard. Precision and calibration of data were monitored through routine analysis of the IAEA NBS-19 standard. Standard deviation for $\delta^{13}C$ and $\delta^{18}O$ are ±0.05‰ and ±0.10‰, respectively (one sigma). Isotopic data are reported in table 1.

Results

A detailed discussion of the lithology of Clinton and Lockport Group strata is beyond the scope of this investigation and has been well documented elsewhere (e.g. Brett et al. 1995; Brett and Goodman 1996; Brett 1999). The stratigraphic column of the sampled interval is shown in text-figure 3 together with the carbon isotope data. Strata from the upper part of the Clinton through the Lockport contain a range of carbonate lithofacies from black shales to reefs to vuggy dolomite. The Williamson Shale marks the initiation of deposition of the upper part of the Clinton with a thin black shale in the study area. Above the Williamson Shale are the Rockway Dolomite and Irondequoit Limestone, which together contain the majority of the Ireviken Extinction Event (Jeppsson 1997a). The second phase of shale deposition in the Appalachian Basin is represented by the Rochester Shale, which can be recognized in the subsurface as a pronounced peak in gamma ray logs (>100API; Brett et al. 1995). An interval of shallowing above the Rochester Shale has long been recognized in the overlying Decew Dolomite. A sequence bounding unconformity separates the DeCew from overlying grainstones of the Gasport Formation, which shows renewed transgression into the reefal muddy carbonate facies. A further subaerial unconformity lies at the base of the Goat Island Formation. Extensive thrombolitic bioherms in the Eramosa Formation indicate continued shallowing into restricted lagoonal facies.

Carbon isotope values in the Williamson and lower Rockway Formations of ~+3.0‰ represent the elevated baseline values prior to the Ireviken Excursion. The sharp increase in $\delta^{13}C_{carb}$ values (+2.9‰ to +5.5‰), near the disconformable Rockway-Irondequoit contact, represents the largest rate of change in the sampled interval and marks the onset of the Ireviken Excursion. This conclusion is supported by the fact that the conodont *P. amorphognathoides* is known to have its highest stratigraphic occurrence in upper-Rockway/lower-Irondequoit strata. The entirety of the Ireviken Extinction event has not been clearly identified in the study area and may in fact be partially missing due to erosion or non-deposition at the basal Irondequoit contact (Brett et al. 1990). This could account for the sharp increase in values near the Rockway-Irondequoit contact.

Apart from a small decrease in values in the lower Rochester, $\delta^{13}C_{carb}$ values remain very close to +5.0‰ well into the Gasport Formation. The return to baseline values of +2.5‰ in the lower Goat Island Formation represents the end of the Ireviken Excursion. The conclusion that the Ireviken Excursion ends in the Goat Island is supported by the fact that the conodont *Ozarkodina sagitta rhenana* has its highest stratigraphic occurrence in the upper Goat Island above the onset of the decline in $\delta^{13}C_{carb}$ values. The Ireviken Excursion is known to end within the Lower *K. walliseri* Zone (Calner et al. 2004), the top of which is marked by the extinction of *O. s. rhenana* (Jeppsson 1997a). The steady decline in $\delta^{13}C_{carb}$ values well after the end of the Ireviken Excursion, in the uppermost Goat Island through Eramosa of nearly -5.0‰, has previously never been documented, even though this interval of Silurian time has been well

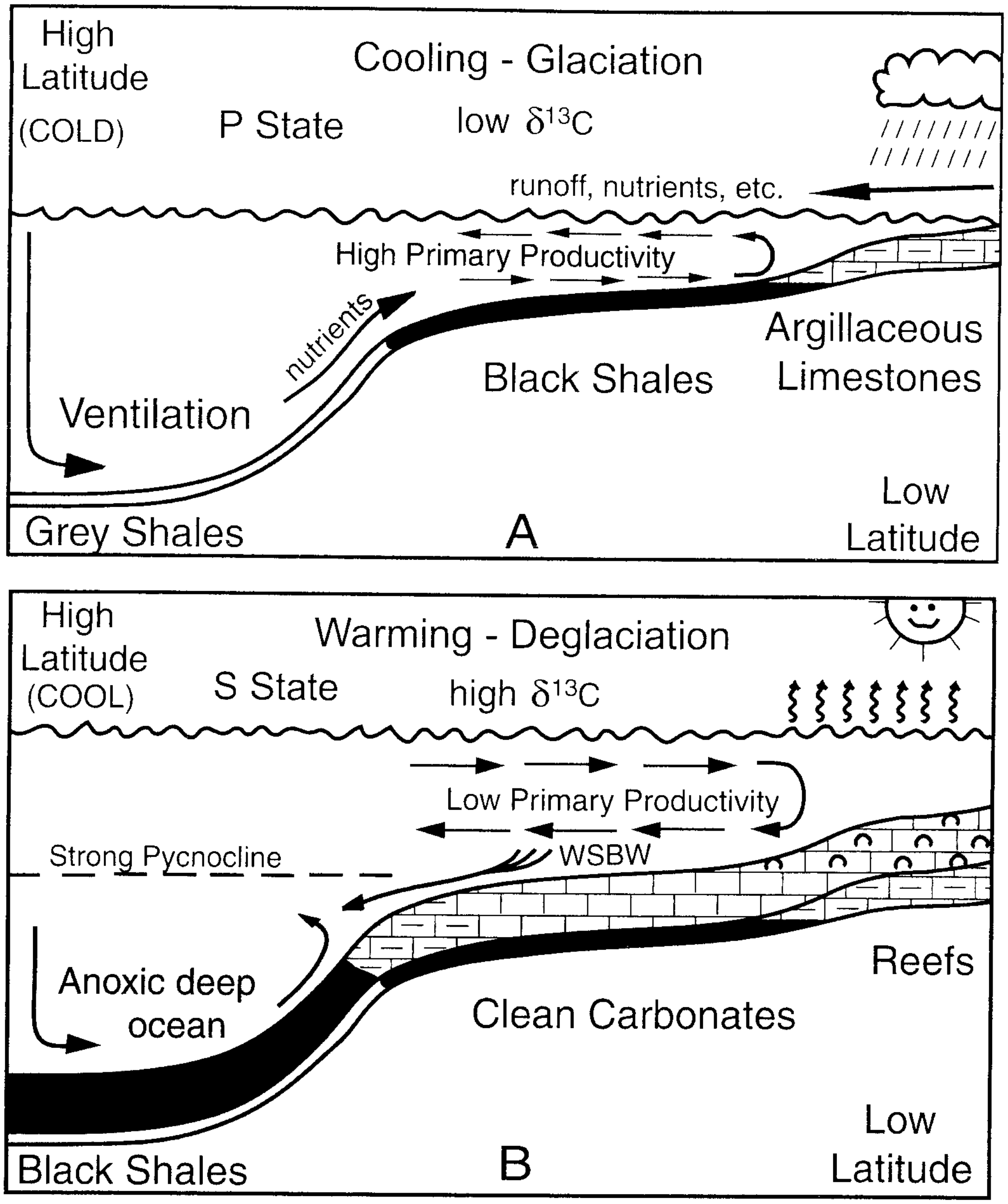

TEXT-FIGURE 5
Paleoceanographic reconstruction for the late Llandovery (A) and the early Wenlock (B). Diagram modified from Cramer and Saltzman (2005) originally modified from Jeppsson (1990) and Bickert et al. (1997). Note the transition from estuarine circulation on the shelf in A to anti-estuarine circulation ("quasi-estuarine" circulation of Witzke, 1987) during B. Black shales in A are located in epicontinental seas as a result of high primary productivity while black shales in B are the result of deep ocean anoxia produced by a change in the site of deep water formation from high to low latitudes; WSBW=Warm Saline Bottom Water.

sampled elsewhere. Therefore we can not rule out local effects ("aging" a restricted watermass: Patterson and Walter 1994) without global confirmation of this negative shift.

DISCUSSION

The Sheinwoodian (Ireviken) positive carbon isotope excursion is recorded in strata from the type area of the Niagaran Provincial Series in western New York. The revised correlation of Appalachian Basin stratigraphy provided by the data presented herein demonstrates an important feature of epeiric sea oceanography. We first discuss the timing of epicontinental organic-carbon deposition with respect to the Ireviken Excursion. We then address the significance of the revised correlation of Clinton and Lockport strata in the context of an oceanographic model for the Silurian that relates spatial and temporal changes in the location of organic carbon burial to changes in global oceanography driven by alternations between cold and warm climate states.

Eustatic change across the Llandovery-Wenlock boundary

The well-documented Late Ordovician icehouse interval, which may have begun as early as the Caradoc (Pope and Steffen 2003; Saltzman and Young 2005) continued well into the Silurian with several intervals of early Silurian glaciation known from deposits in South America (Díaz-Martínez 1998; Caputo 1998). Evidence of a late Llandovery (late Telychian) uncon-

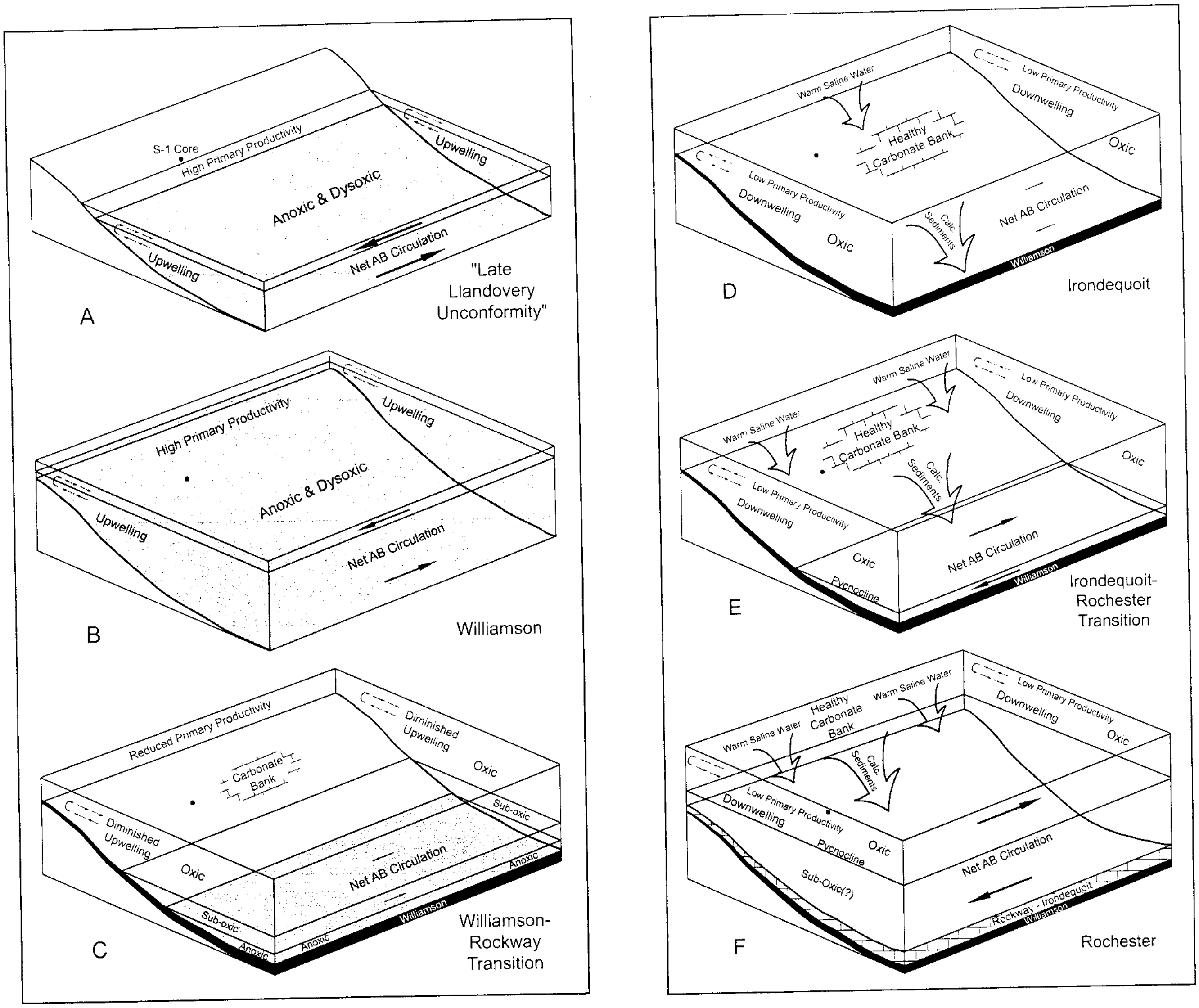

TEXT-FIGURE 6
Detailed application of the model shown in text-figure 5 to Llandovery-Wenlock Boundary times in the Appalachian Basin. The arrows on the southeast facing vertical profile represent the net motion of waters in the AB along its axis. The small arrows on the southwest facing vertical profile, depicting upwelling or downwelling, are the Ekman result of the flow of surface waters in the AB. When the surface layer of the AB is flowing to the southwest (A, B, and C), the northwest margin of the basin experienced upwelling as surface waters were pulled away from the arches. When the surface layer of the AB was flowing to the northeast, surface waters were pushed towards the arches replacing saline downwelled water. Note the difference in timing and location of the two periods of anoxia and consequent shale deposition: Transgressive black shales in epeiric seas resulting from primary productivity induced anoxia (Williamson Shale) *vs* highstand shales in deep intracratonic basins and the deep ocean resulting from sluggish poorly oxygenated bottom water production (oceanographically induced anoxia). Deep intra-cratonic basins such as the Appalchian Basin experienced increased organic carbon burial (Rochester Shale) due to decreased ventilation and elevated sedimentation rates resulting from a healthy carbonate factory throughout epeiric seas. See text for detailed discussion of each time slice.

formity is present throughout North America from Nevada to Wisconsin to Tennessee to New York (Murphy et al. 1979; Barrick 1983; Brett et al. 1990; Goodman and Brett 1994; Kluessendorf and Mikulic 1996). Although this sea-level fall has been interpreted either as a eustatic and tectonic event, the presence of late Telychian glacial deposits throughout South America (Díaz-Martínez 1997; 1998) supports a glacio-eustatic origin for this sea level fall.

The fact that elevated $\delta^{13}C_{carb}$ values indicative of the Ireviken Excursion are recorded following the late Llandovery unconformity throughout the mid-continent of North America (Saltzman 2001; Cramer and Saltzman 2005) indicates that transgression continued during the rising limb of the Ireviken Excursion, which closely tracks a third order T-R cycle (text-fig 4). It is interesting to note that clearly global, higher order sea-level cyclicity took place within the large scale eustatic change shown in text-figure 4 (compare Cramer and Saltzman 2005, fig. 9 with Eriksson and Calner 2005, fig. 10). It remains unclear why these higher order eustatic changes had little to no impact on the Ireviken Excursion.

Organic carbon burial during the Ireviken interval

The realization that major Paleozoic positive carbon isotope excursions typically occur during an expansion of reef and car-

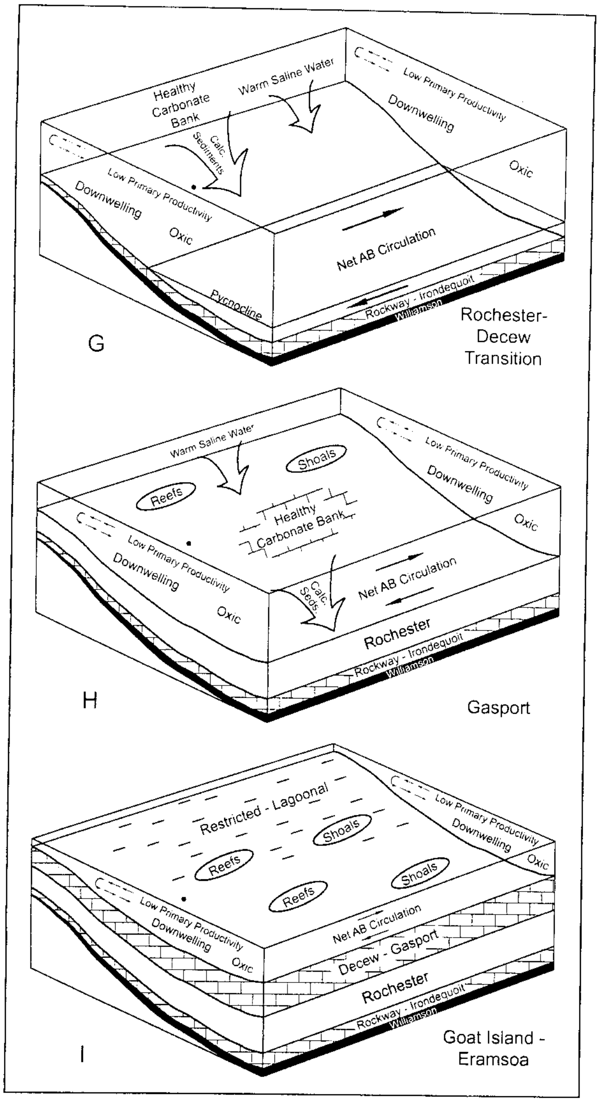

TEXT-FIGURE 6
Continued.

bonate platform environments in epeiric seas has promoted a renewed search for the location of organic carbon sequestration and burial during these events (e.g. Munnecke et al. 2003). It has been suggested (Bickert et al. 1997; Cramer and Saltzman 2005) that organic carbon sequestration took place in the deep ocean during the Ireviken Excursion. Unfortunately, lower Paleozoic abyssal sediments are generally unavailable, which has hindered further testing of this hypothesis. According to Cramer and Saltzman (2005), the Ireviken Excursion was the result of deep ocean anoxia, driven by the production of saline bottom water in low-mid latitude epeiric seas. Below, we show how the Appalachian Basin sequence demonstrates for the first time the increased production of saline waters in epeiric seas during the Ireviken Excursion.

Two intervals of dysoxic mud deposition occurred in the Appalachian Basin during the interval of the Silurian sampled in this investigation, neither of which is responsible for the Ireviken Excursion itself. The first is represented by the late Telychian Williamson Shale, which precedes the Ireviken Excursion. The second is represented by the early Sheinwoodian Rochester Shale, which is coincident with peak $\delta^{13}C_{carb}$ values during the middle of the Ireviken Excursion. The late Telychian interval of epicontinental organic carbon deposition (Williamson Shale) is known to be a global phenomenon (Lüning et al. 2000a; Lüning et al. 2000b) with economically important "hot" shales throughout North Africa and Arabia. The early Sheinwoodian dysoxic interval in the Appalachian Basin (Rochester Shale) is exceptional when compared with platform and ramp settings, contrasting greatly with the intense reef building and expansion of carbonate platforms seen throughout the low-mid latitudes during this time (Brunton et al. 1998; Calner et al. 2004). The oceanographic model first developed by Jeppsson (1990) and later expanded by Cramer and Saltzman (2005) accounts for the timing and location of both intervals of dysoxic deposition, and connects them to changes in global oceanography driven by alternations between climate states.

Ireviken Oceanography

According to Jeppsson (1998), the Silurian can be divided into over 20 alternating climatic episodes and intervening extinction events. Referred to as Primo and Secundo (P and S), these climate states resemble short term (1-4 myr) icehouse-greenhouse intervals. A well developed latitudinal thermal gradient and predisposition for polar glaciation promoted vigorous thermohaline circulation and lower sea level during P states. Climatic optima during S states produced polar warming, increased sea level, diminished thermohaline circulation and upwelling, and occasionally induced salinity-driven halothermal circulation, all of which were conducive to epeiric sea carbonate production (Hallock 1988; 2001; Rankey 2004; Halfar et al. 2004). An expanded version of the model (Cramer and Saltzman 2005) is shown in text-figure 5.

The sequence of oceanographic and eustatic changes responsible for the Ireviken Excursion and the stratigraphy of the study area as developed in the Silurian model are illustrated in several time slices (text-fig. 6). Text-figure 6A represents low-stand conditions during glaciation and the initial pulse of deglaciation. Intense polar downwelling due to a well developed equator to pole thermal gradient drove vigorous thermohaline circulation, which delivered copious levels of nutrients to the upper water column. The AB (Appalachian Basin) was connected to the deep-ocean by the region between the southern extent of the Taconic Highlands to the southeast and the Nashville Dome to the southwest of the study area. Coupled with the large river systems that fed into the northeastern Appalachian Basin, which would have pushed a freshwater lens to the southwest, the AB experienced net estuarine circulation (Witzke 1987; Bickert et al. 1997) with bottom water flowing in from the southwest and surface waters flowing out from the northeast. A surface layer flowing to the southwest would induce Ekman upwelling on the northwest side of the basin as water was pulled away from the Findlay and Algonquin Arches towards the AB. The consequent high nutrient availability promoted primary productivity to the point that large portions of the basin became anoxic. The Williamson Shale was deposited in dysoxic to anoxic conditions (e.g. Eckert and Brett 1989) under high productivity waters. Alignment of graptolites within the Williamson Shale in the NE-SW direction (O'Brien et al. 1998), indicates that the black shales were deposited in waters that had at least a minimal amount of bottom current. This further suggests that the shales of the Williamson were not the product of bottom water stagnation alone. This global interval of high primary productivity began during the late stages of glaciation and the initial onset of deglaciation. As rapid transgression progressed (text-fig. 6B) intense upwelling in the deep ocean and the AB (although both were constantly diminishing) continued, depositing a thin layer of Williamson in the study area. Our depositional model for the Williamson Shale is similar to the "deglacial" black shales of Armstrong et al. (2005) as well as the model presented in Lüning et al. (2000b).

Text-figure 6C depicts oceanographic conditions immediately prior to the onset of deposition of the Rockway Formation. As deglaciation progressed, the intense equator to pole thermal gradient was rapidly diminishing, severely weakening polar downwelling and thermohaline circulation as well as decreasing nutrient delivery to surface waters from depth. The consequent reduction in primary productivity required less oxygen for decomposition of organic matter, which allowed a progressive oxygenation of the basin. The Rockway Formation was deposited under these transitional conditions as surface waters in the northern end of the AB switched from nutrient-rich to nutrient-poor conditions. Transgression of the Laurentian craton produced a tremendous area for the production of saline water, which combined with the decline in thermohaline circulation to induce a transition to downwelling off the cratons with saline waters initially sinking to the deepest regions of epeiric seas, such as the Appalachian Basin.

The Irondequoit Limestone (text-fig. 6D) was deposited following a major shallowing that produced a sharp sequence boundary at the top of the Rockway Formation. This event, in early Sheinwoodian time coincides with the initiation of the Ireviken Excursion as saline waters downwelling off the craton into the deep ocean progressively disconnected the deep ocean reservoir of light carbon from epicontinental seas. As transgression was initiated following the sequence boundary (text-fig. 6E) and saline bottom water production intensified, a strong pycnocline began to develop in the deepest parts of the Appalachian Basin as sinking saline water collected in the deepest parts of the craton (this is the same as the pycnocline shown in text-figure 5B only in an intra-cratonic basin setting as opposed to the open ocean). The growing deep saline water-mass in the AB began to flow out to the southwest, intensifying anti-estuarine circulation in the basin. To maintain water balance, surface waters must have been coming in from the southwest, which through Ekman transport would have pushed water inshore towards the Findlay and Algonquin Arches, replacing waters downwelled off the arches.

Further transgression during Rochester Shale deposition, almost completely flooded the Laurentian craton, and the continued downwelling of deep saline water into the Appalachian Basin served to intensify the pycnocline driving it to shallower depths below the sea surface (text-fig. 6F). At this point it is unclear if the water beneath this pycnocline was occasionally sub-oxic due to epeiric sea oceanography and the limited amount of oxygen in warm tropical waters (e.g. Herbert and Sarmiento 1991) or if the huge amount of carbonate material being shed off a craton-sized healthy carbonate factory increased sedimentation rates so much that organic carbon had little time to be oxidized at the sediment water interface (e.g. Bralower and Thierstein 1984). What is clear however, is that dysoxic mud deposition in the AB increased during deposition of the Rochester Shale. The AB during deposition of the Rochester was certainly oxygenated at least in shallower areas as indicated by benthic communities *in situ* within the Rochester Formation (Brett 1999) however, both the Rochester and laterally equivalent Osgood Shale show unusually abrupt transitions from richly fossiliferous beds to nearly barren gray mudstones, which indicates a strongly defined pycnocline. Surprisingly, the barren facies are not comprised of laminated, organic rich shales and Brett (1999) suggested that the deeper waters may have been hypersaline. It is likely that the pycnocline would have fluctuated seasonally, annually, and on many other time-scales, and this issue certainly deserves further investigation. For this study however, we have interpreted the Rochester to reflect the most intense interval of saline bottom water delivery into the AB when a well-developed pycnocline and increased sedimentation rates acted to stagnate deeper waters in a low-productivity setting leading to the deposition of the dysoxic mud.

The deep-ocean organic carbon burial responsible for the Ireviken Excursion eventually acted to lower atmospheric CO_2 concentrations (Berner and Kothavala 2001) decreasing global temperatures and initiating a eustatic drop in sea level. As regression began (text-fig. 6G), saline deep water production continued, but was diminishing as the flooded portion of Laurentia began to be reduced and global temperatures began to decline. Coupled with the reduction of accommodation space in the AB, the well developed pycnocline began to sink and eventually disappear. The lowering of sea level brought the storm debris, soft sediment deformation, and hummocky cross stratification of the DeCew Formation, which was sourced by a healthy carbonate bank soon to prograde across the basin. Continued regression (text-fig. 6H) brought about exposure and development of a sequence boundary (Brett et al. 1990).

Renewed transgression during deposition of the Lockport Group led to establishment of a healthy carbonate bank in the study area followed closely by reefs and carbonate shoals of the Gasport Formation as the AB became a site of formation instead of a depo-center for saline deep water. Downwelling continued as the AB became more restricted although saline water production had already begun to decline. The reduction in saline water production and downwelling was a global phenomenon that signaled the beginning of the end for the Ireviken Excursion. Lowering of sea level following Gasport deposition and a new episode of transgression (text-fig. 6I) brought continued reef and carbonate shoal deposition (Goat Island).

Correlation outside the Appalachian Basin and oceanographic implications

Precise correlation of Upper Clinton and Lockport Group strata with global sections containing the Ireviken Excursion is now possible. Deposition during the transgression recorded above the "Late Llandovery Unconformity" of Murphy et al. (1979) began at different times across the Laurentian craton where the Llandovery-Wenlock boundary was only recorded in deep sections and is often not present in shallower settings. In all suitably detailed and sufficiently correlated sections, the strata between the Late Llandovery Unconformity and the onset of the Ireviken Excursion (dark grey band in text-fig. 7) show the hallmarks of vigorous thermohaline circulation and intense nutrient delivery to shallow water. Cherts along the eastern margin of the Panthalassic Ocean (Murphy et al. 1979), epicontinental black shales along the northern margin of Gondwana resulting from intense Southern Hemisphere Westerlies (Parrish 1982; Moore et al. 1993; Lüning et al. 2000a; Lüning et al. 2000b), as well as phosphate lags, ironstones, and black shales of the Appalachian Basin (Goodman and Brett 1994; Brett et al. 1998) are all features indicative of an increased latitudinal thermal

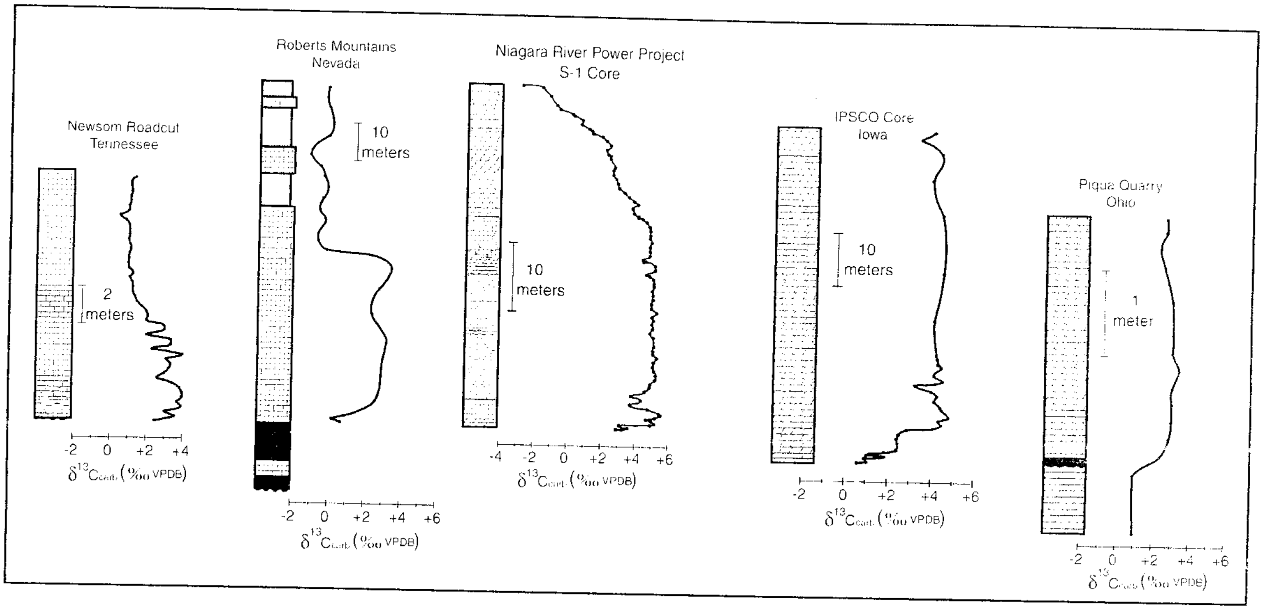

TEXT-FIGURE 7
Chemostratigraphic correlation of the sampled section with the data presented in Saltzman (2001) and Cramer and Saltzman (2005). The dark grey band represents strata between the "Late Llandovery Unconformity" and the onset of the Ireviken Excursion. The light grey band represents only the Ireviken Excursion. The lack of a gentle decline in the Nevada section is likely the result of a fault at the top of the excursion in the sampled section.

gradient and vigorous deep circulation. The Williamson Shale is the local expression of this global episode of intense organic carbon burial in shallow epicontinental settings immediately prior to the Ireviken Excursion.

The Ireviken Excursion itself (light grey band in text-fig. 7) occurred after the high organic carbon burial in epicontinental seas and is most frequently noted for its coincidence with an episode of prolific reef development and expansion of carbonate platforms throughout low-mid latitude epeiric seas (Bickert et al. 1997; Brunton et al. 1998; Cramer and Saltzman 2005). The change from Williamson and Rockway shaley units into the Irondequoit pack- to grainstones interval records the familiar shale to carbonate transition that so often marks the Llandovery-Wenlock transition (Jeppsson et al. 1995; Brunton et al. 1998). Peculiar barren, dysoxic facies of the Rochester shale are a necessary and predicted outcome of the Silurian oceanographic model discussed herein and attest to the production of downwelling saline waters in epeiric seas during the Ireviken Excursion. If the Ireviken Excursion was the result of sequestration and burial of ^{12}C in the deep ocean resulting from a change in the site of deep water formation from high to low latitudes (Cramer and Saltzman 2005), then peak $\delta^{13}C_{carb}$ values during the Ireviken Excursion should be coincident with maximum saline water-mass production (Rochester Shale). As the size of the saline water-mass sinking off the cratons diminished during the initial stages of global cooling and regression, halothermal circulation in the global ocean began to weaken while polar cooling and a re-establishment of the equator to pole thermal gradient strengthened thermohaline circulation, progressively oxygenating the deep ocean, reconnecting shallow epeiric seas with the deep ocean carbon reservoir, and ending the Ireviken Excursion.

SUMMARY AND CONCLUSIONS

By illustrating that the peculiar facies of the Rochester Shale were coincident with the Ireviken Excursion, we have demonstrated an important prediction made by the original model (Jeppsson 1990); namely, the production of saline bottom waters in epeiric seas. That saline bottom water was being produced in the cratonic interior and downwelled into interior basins during the Ireviken Excursion provides support for the oceanographic model presented in Cramer and Saltzman (2005) where a change in the site of bottom water formation from high to low latitudes was suggested to be the cause of the Ireviken Excursion.

Elevated baseline $\delta^{13}C_{carb}$ values immediately prior to the Ireviken Excursion are the result of intense organic carbon burial in shallow epicontinental seas during transgression. This initial episode of organic carbon burial was the result of intense deep upwelling and elevated primary productivity, and it is not responsible for nor does it coincide with the Ireviken Excursion. The second episode of organic carbon sequestration and burial took place in the deep ocean as saline waters downwelling from the cratons induced deep ocean anoxia and progressively disconnected epeiric seas from the deep ocean reservoir of carbon. The Rochester Shale was an unusual mudrock facies that accumulated around the margins of a density stratified hypersaline and low productivity basin. Organic carbon burial during the excursion was limited to the deep ocean and the deepest of intra-cratonic basin settings where a well developed pycnocline and high sedimentation rates combined to increase organic carbon burial in low productivity settings.

The high resolution carbon isotope ($\delta^{13}C_{carb}$) data presented in this study demonstrate the potential of $\delta^{13}C_{carb}$ stratigraphy as a correlation tool and provide insight into the role of epicontinental organic carbon burial in positive carbon isotope excursions. It is only through high-resolution $\delta^{13}C_{carb}$ stratigraphy that the subtle variations in the location and timing of organic carbon burial associated with the Ireviken Excursion (and perhaps most Paleozoic excursions) can be deciphered, and to that end, much more work still needs to be done. Ideally, shelf to basin transects through major positive carbon isotope excursions

TABLE 1
Stable isotope data, Niagara River Power Project S-1, Lewiston, New York.

Stable Isotope Data, Niagara River Power Project S-1 Core, Lewiston, NY

ft. downcore	meters*	$\delta^{13}C$	$\delta^{18}O$	Conodont Zone/Superzone/Zonal Group	Formation	Member
11	49.62	-2.89	-6.19	*K. O. ortus Superzone(?)*	Eramosa	
12	49.32	-1.68	-6.48	*K. O. ortus Superzone(?)*	Eramosa	
16	48.10	-1.23	-6.73	*K. O. ortus Superzone(?)*	Eramosa	
20	46.88	-0.83	-7.42	*K. O. ortus Superzone(?)*	Eramosa	
22	46.27	-0.64	-6.42	*K. O. ortus Superzone(?)*	Eramosa	
24	45.66	0.09	-6.43	*K. O. ortus Superzone(?)*	Eramosa	
25	45.35	0.20	-6.63	*K. O. ortus Superzone(?)*	Eramosa	
27	44.74	0.70	-4.49	*K. O. ortus Superzone(?)*	Eramosa	
29	44.14	0.64	-4.24	*K. O. ortus Superzone(?)*	Eramosa	
31	43.53	1.10	-4.15	*K. O. ortus Superzone(?)*	Eramosa	
32	43.22	1.21	-4.16	*K. O. ortus Superzone(?)*	Eramosa	
33	42.92	1.30	-3.68	*Upper K. walliseri Superzone(?)*	Goat Island	Vinemount
35	42.31	1.85	-4.73	*Upper K. walliseri Superzone(?)*	Goat Island	Vinemount
37	41.70	2.12	-5.41	*Upper K. walliseri Superzone(?)*	Goat Island	Vinemount
39	41.09	2.35	-5.55	*Upper K. walliseri Superzone(?)*	Goat Island	Vinemount
41	40.48	2.13	-5.71	*Upper K. walliseri Superzone(?)*	Goat Island	Vinemount
43	39.87	2.19	-4.40	*Upper K. walliseri Superzone(?)*	Goat Island	Vinemount
44	39.56	2.34	-3.43	*Upper K. walliseri Superzone(?)*	Goat Island	Vinemount
45	39.26	2.35	-4.11	*Upper K. walliseri Superzone(?)*	Goat Island	N.F. and Ancaster
47	38.65	0.17	-6.42	*Upper K. walliseri Superzone(?)*	Goat Island	N.F. and Ancaster
49	38.04	2.62	-3.52	*Upper K. walliseri Superzone(?)*	Goat Island	N.F. and Ancaster
51	37.43	2.53	-5.00	*Lower K. walliseri Zone*	Goat Island	N.F. and Ancaster
53	36.82	2.52	-4.64	*Lower K. walliseri Zone*	Goat Island	N.F. and Ancaster
55	36.21	2.69	-3.41	*Lower K. walliseri Zone*	Goat Island	N.F. and Ancaster
57	35.60	2.80	-5.45	*Lower K. walliseri Zone*	Goat Island	N.F. and Ancaster
59	34.99	2.90	-5.94	*Lower K. walliseri Zone*	Goat Island	N.F. and Ancaster
61	34.38	3.23	-5.39	*Lower K. walliseri Zone*	Goat Island	N.F. and Ancaster
63	33.77	3.49	-5.92	*Lower K. walliseri Zone*	Goat Island	N.F. and Ancaster
65	33.16	3.80	-5.61	*Lower K. walliseri Zone*	Goat Island	N.F. and Ancaster
67	32.55	4.01	-5.37	*Lower K. walliseri Zone*	Goat Island	N.F. and Ancaster
69	31.94	3.71	-4.02	*Lower K. walliseri Zone*	Goat Island	N.F. and Ancaster
71	31.33	3.80	-3.99	*Lower K. walliseri Zone*	Goat Island	N.F. and Ancaster
72	31.03	4.04	-4.82	*Lower K. walliseri Zone*	Goat Island	N.F. and Ancaster
73	30.72	4.08	-4.66	*Lower K. walliseri Zone*	Goat Island	N.F. and Ancaster
74	30.42	4.34	-4.88	*Lower K. walliseri Zone*	Gasport	Pekin
75	30.11	4.54	-4.05	*Lower K. walliseri Zone*	Gasport	Pekin
77	29.50	4.76	-5.99	*Lower K. walliseri Zone*	Gasport	Pekin
79	28.90	4.77	-7.56	*Lower K. walliseri Zone*	Gasport	Pekin
81	28.29	4.78	-7.43	*Lower K. walliseri Zone*	Gasport	Pekin
83	27.68	4.79	-8.66	*Lower K. walliseri Zone*	Gasport	Pekin
85	27.07	4.86	-8.48	*Lower K. walliseri Zone*	Gasport	Pekin
87	26.46	4.80	-8.83	*Lower K. walliseri Zone*	Gasport	Pekin
89	25.85	4.78	-8.42	*Lower K. walliseri Zone*	Gasport	Gothic Hill
91	25.24	4.79	-6.74	*Lower K. walliseri Zone*	Gasport	Gothic Hill
93	24.63	4.39	-8.10	*Lower K. walliseri Zone*	Gasport	Gothic Hill
93.8	24.38	4.56	-6.98	*Lower K. walliseri Zone*	Gasport	Gothic Hill

* Meters above the base of the Williamson-Rockway contact

will be carried out to investigate this paleoceanographic model further. We have hopefully demonstrated the need for precise correlation of global sections before any interval of organic-rich deposit can be positively identified as being "responsible" for a positive carbon isotope excursion.

ACKNOWLEDGMENTS

We would like to thank two anonymous reviewers who greatly improved this manuscript. Rose Schulze and Rich Nyahay at the New York State Museum provided invaluable assistance and access to the core. We would like to thank L. Fay (The Ohio State University) for assistance with sampling, C. Brett (University of Cincinnati) for assistance with the Appalachian Sequence, and T. Prokopiuk (University of Saskatchewan) for expeditious lab work. This work is a contribution to the IGCP 503 project and the result of discussions held at the IGCP 503 meeting in Erlangen Germany.

TABLE 1
Continued.

Stable Isotope Data, Niagara River Power Project S-1 Core, Lewiston, NY

ft. downcore	meters*	$\delta^{13}C$	$\delta^{18}O$	Conodont Zone/Superzone/Zonal Group	Formation	Member
94	24.32	4.42	-7.59	Lower *K. walliseri* Zone	DeCew	
96	23.71	5.11	-6.70	Lower *K. walliseri* Zone	DeCew	
98	23.10	5.09	-5.75	Lower *K. walliseri* Zone	DeCew	
100	22.49	4.61	-4.70	Lower *K. walliseri* Zone	DeCew	
101	22.19	4.80	-5.07	Lower *K. walliseri* Zone	DeCew	
102	21.88	5.01	-4.90	Lower *K. walliseri* Zone	DeCew	
104	21.28	5.07	-4.29	*O. s. rhenana* Zone	Rochester	Burleigh Hill
106	20.67	5.05	-4.45	*O. s. rhenana* Zone	Rochester	Burleigh Hill
108	20.06	4.98	-3.66	*O. s. rhenana* Zone	Rochester	Burleigh Hill
110	19.45	5.02	-3.58	*O. s. rhenana* Zone	Rochester	Burleigh Hill
112	18.84	5.01	-4.47	*O. s. rhenana* Zone	Rochester	Burleigh Hill
114	18.23	4.91	-5.40	*O. s. rhenana* Zone	Rochester	Burleigh Hill
116	17.62	4.94	-5.20	*O. s. rhenana* Zone	Rochester	Burleigh Hill
118	17.01	5.22	-5.06	*O. s. rhenana* Zone	Rochester	Burleigh Hill
120	16.40	4.96	-5.53	*O. s. rhenana* Zone	Rochester	Burleigh Hill
122	15.79	5.03	-5.20	*O. s. rhenana* Zone	Rochester	Burleigh Hill
124	15.18	4.95	-5.42	*O. s. rhenana* Zone	Rochester	Burleigh Hill
126	14.57	4.99	-4.76	*O. s. rhenana* Zone	Rochester	Burleigh Hill
128	13.96	4.88	-5.34	*O. s. rhenana* Zone(?)	Rochester	Burleigh Hill
130	13.35	5.04	-4.52	*O. s. rhenana* Zone(?)	Rochester	Lewiston
132	12.74	1.89	-4.09	*O. s. rhenana* Zone(?)	Rochester	Lewiston
134	12.13	5.08	-5.26	*O. s. rhenana* Zone(?)	Rochester	Lewiston
136	11.52	5.07	-5.74	*K. ranuliformis* Superzone(?)	Rochester	Lewiston
138	10.91	5.04	-5.82	*K. ranuliformis* Superzone(?)	Rochester	Lewiston
140	10.30	5.30	-5.43	*K. ranuliformis* Superzone	Rochester	Lewiston
142	9.69	5.12	-7.10	*K. ranuliformis* Superzone	Rochester	Lewiston
144	9.08	5.07	-7.05	*K. ranuliformis* Superzone	Rochester	Lewiston
146	8.47	5.14	-6.12	*K. ranuliformis* Superzone	Rochester	Lewiston
148	7.86	5.23	-5.83	*K. ranuliformis* Superzone	Rochester	Lewiston
150	7.25	5.17	-5.93	*K. ranuliformis* Superzone	Rochester	Lewiston
152	6.64	4.90	-6.69	*K. ranuliformis* Superzone	Rochester	Lewiston
154	6.04	4.86	-5.87	*K. ranuliformis* Superzone	Rochester	Lewiston
156	5.43	4.61	-6.60	*K. ranuliformis* Superzone	Rochester	Lewiston
158	4.82	3.81	-7.59	*K. ranuliformis* Superzone	Rochester	Lewiston
160	4.21	4.36	-5.53	*K. ranuliformis* Superzone	Rochester	Lewiston
162	3.60	3.74	-6.36	*K. ranuliformis* Superzone	Irondequoit	
164	2.99	4.79	-4.94	*K. ranuliformis* Superzone	Irondequoit	
166	2.38	5.47	-3.35	*K. ranuliformis* Superzone	Irondequoit	
167	2.07	5.55	-4.54	*K. ranuliformis* Superzone	Irondequoit	
168	1.77	5.24	-4.08	*K. ranuliformis* Superzone	Irondequoit	
169	1.46	4.68	-5.59	*K. ranuliformis* Superzone	Irondequoit	
170	1.16	4.99	-4.50	*K. ranuliformis* Superzone(?)	Irondequoit	
171	0.85	5.18	-4.05	Upper *Pterospathodus* Zonal Group(?)	Rockway	
171.5	0.70	4.98	-4.85	Upper *Pterospathodus* Zonal Group	Rockway	
172	0.55	3.12	-5.36	Upper *Pterospathodus* Zonal Group	Rockway	
173	0.24	3.61	-8.48	Upper *Pterospathodus* Zonal Group	Rockway	
173.8	0.00	2.96	-4.75	Upper *Pterospathodus* Zonal Group	Williamson	
174	-0.06	3.24	-4.98	Upper *Pterospathodus* Zonal Group	Williamson	

* Meters above the base of the Williamson-Rockway contact

REFERENCES

ARMSTRONG, H.A., TURNER, B.R., MAKHLOUF, I.M., WEEDON, G.P., WILLIAMS, M., AL SMADI, A., SALAH, A.A., 2005. Origin, sequence stratigraphy, and depositional environment of an upper Ordovician (Hirnantian) deglacial black shale, Jordan. *Palaeogeography, Palaeoclimatology, Palaecology*, in press. doi: 10.1016/j.palaeo.2005.01.007.

ARTHUR, M.A., SCHLANGER, S.O., and JENKYNS, H.C., 1987. The Cenomanian-Turonian oceanic anoxic event II: Palaeoceanographic controls on organic matter production and preservation. In: Brooks, J., and Fleet, A.J., Eds. *Marine Petroleum Source Rocks*, 401-420. Geological Society of London Special Publication, 26.

AZMY, K., VEIZER, J., BASSETT, M.G., and COPPER, P., 1998. Oxygen and carbon isotopic composition of Silurian brachiopods: Implications for coeval seawater and glaciations. *Geological Society of America Bulletin,* 110:1499-1512.

BAARLI, B.G., 1998. Silurian cycles and proximality-trend analysis of tempestite deposits. In: Landing, E., and Johnson, M.E., Eds. Silurian cycles: Linkages of dynamic stratigraphy with atmospheric, oceanic and tectonic changes. *New York State Museum Bulletin,* 491:75-88.

BANNER, J.L., and HANSON, G.N., 1990. Calculation of simultaneous isotopic and trace element variations during water-rock interaction with applications to carbonate diagenesis. *Geochimica et Cosmochimica Acta,* 54:3123-3137.

BARRICK, J.E., 1983. Wenlockian (Silurian) conodont biostratigraphy, biofacies, and carbonate lithofacies, Wayne formation, Central Tennessee. *Journal of Paleontology,* 57:208-239.

BERNER, R.A., and CANFIELD, D.A., 1989. A model for atmospheric oxygen over Phanerozoic time. *American Journal of Science,* 289:333-361.

BERNER, R.A., and KOTHAVALA, Z., 2001. GEOCARB III: A revised model of atmospheric CO2 over Phanerozoic time. *American Journal of Science,* 301:182-204.

BERRY, W.B.N., 1998. Silurian oceanic episodes: The evidence from central Nevada. *New York State Museum Bulletin,* 491:259-264.

BERRY, W.B.N., and BOUCOT, A.J., 1970. *Correlation of the North American Silurian rocks.* Boulder, CO: Geological Society of America Special Paper, 102.

BICKERT, T., PÄTZOLD, J., SAMTLEBEN, C., and MUNNECKE, A., 1997. Paleoenvironmental changes in the Silurian indicated by stable isotopes in brachiopod shells from Gotland, Sweden. *Geochimica et Cosmochimica Acta,* 61:2717-2730.

BRALOWER, T.J., and THIERSTEIN, H.R., 1984. Low productivity and slow deep-water circulation in mid-Cretaceous oceans. *Geology,* 12:614-618.

BRAND, U., LEGRAND-BLAIN, M., and STREEL, M., 2004. Biochemostratigraphy of the Devonian-Carboniferous boundary global Stratotype section and point, Griotte Formation, La Serre, Montagne Noire, France. *Palaeogeography, Palaeoclimatology, Palaeoecology,* 205:337-357.

BRETT, C.E., 1999. Wenlockian fossil communities in New York state and adjacent areas. In: Boucot, A.J., and Lawson, J.D., Eds., *Paleocommunities – a case study from the Silurian and Lower Devonian,* 592-637. Cambridge: Cambridge University Press, World and regional Geography 11.

BRETT, C.E., and GOODMAN, W.M., 1996. Upper Ordovician and Silurian sequence stratigraphy and depositional environments in Western New York. *Field guide to the James Hall symposium – second international symposium on the Silurian System,* 178 pp.

BRETT, C.E., GOODMAN, W.M., AND LODUCA, S.T. 1990. Sequences, cycles, and basin dynamics in the Silurian of the Appalachian foreland basin. *Sedimentary Geology* 69:1-52.

BRETT, C.E., TEPPER, D. H., GOODMAN.W.M., LODUCA, S.T., and ECKERT, B-Y, 1995. *Revised stratigraphy and correlation of the Niagaran Provincial Series (Medina, Clinton, and Lockport Groups) in the type area of western New York.* United States Geological Survey Bulletin, 2086, 66 pp.

BRETT, C.E., BAARLI, B.G., CHOWNS, T.M., COTTER, E., DRIESE, S., and JOHNSON, M.E., 1998. Early Silurian condensed horizons, ironstones, and sequence stratigraphy in the Appalachian Foreland Basin. *New York State Museum Bulletin,* 491:89-144.

BRUNTON, F.R., SMITH, L., DIXON, O.A., COPPER, P., KERSHAW, S. and NESTOR, H., 1998. Silurian reef episodes, changing seascapes, and paleobiogeography. *New York State Museum Bulletin,* 491:265-282.

CALNER, M., JEPPSSON, L., and MUNNECKE, A., 2004. The Silurian of Gotland - part 1: review of the stratigraphic framework, event stratigraphy, and stable carbon and oxygen isotope development. *Erlanger Geologische Abhandlungen Sonderband,* 5:113-131.

CAPUTO, M.V., 1998. Ordovician-Silurian glaciations and global sea-level changes. In: Landing, E., and Johnson, M.E., Eds. Silurian cycles: Linkages of dynamic stratigraphy with atmospheric, oceanic and tectonic changes. *New York State Museum Bulletin,* 491:15-25.

CHATTERTON, B.D.E., EDGECOMBE, G.D., and TUFFNELL, P.A., 1990. Extinction and migrationin Silurian trilobites and conodonts of northwestern Canada. *Journal of the Geological Society of London,* 147:703-715.

COCKS, L.R.M., 2001. Ordovician and Silurian global geography. *Journal of the Geological Society of London,* 158:197-210.

CRAMER, B.D., and SALTZMAN, M.R., 2005. Sequestration of 12C in the deep ocean during the early Wenlock (Silurian) positive carbon isotope excursion. *Palaeogeography, Palaeoclimatology, Palaeoecology,* 219:333-349, doi: 10.1016/j.palaeo.2005.01.009.

DÍAZ-MARTÍNEZ, E., 1997. Latest Ordovician-Early Silurian glaciation and carbonate deposition in the Bolivian central Andes. *V Reunión internacional del proyecto 351 del PICG, La Coruña, Libro de Resúmenes y Excursiones,* 51-53.

———, 1998. Silurian of Peru and Bolivia: recent advances and future research. *Temas Geológico-Mineros* ITGE, 23:69-75.

ECKERT, B,-Y., and BRETT, C.E., 1989. Bathymetry and paleoecology of Silurian benthic assemblages, Late Llandoverian, New York State. *Palaeogeography, Palaeoclimatology, Palaeoecology,* 74:297-326.

ERIKSSON, K., and HAGENFELDT, S.E., 1997. Acritarch assemblages from the Lower Silurian (Llandovery-Wenlock) in the Grötlingboborrningen 1 core, Gotland, Sweden. *GFF,* 119:13-16.

ERIKSSON, M.E., and CALNER, M., Eds., 2005. *The dynamic Silurian Earth.* Sveriges geologiska undersökning, Rapporter och meddelanden, 121, 48 pp.

ETTENSOHN, F.R., 1994. Tectonic control on formation and cyclicity of major Appalachian unconformities and associated stratigraphic sequences. In: Dennison, J.M., and Ettensohn; F.R., Eds., *Tectonic and eustatic controls on sedimentary cycles,* 217-242. Society of Economic and Petroleum Mineralogists, Concepts in sedimentology and paleontology, 4.

ETTENSOHN, F.R., and BRETT, C.E., 1998. Tectonic components in Silurian cyclicity: examples from the Appalachian Basin and global implications. *New York State Museum Bulletin,* 491:145-162.

FINNEY, S.C., BERRY, W.B.N., COOPER, J.D., RIPPERDAN, R.L., SWEET, W.C., JACOBSON, S.R., SOUFIANE, A., ACHAB, A., and NOBLE, P.J., 1999. Late Odovician mass extinction: a new perspective from stratigraphic sections in central Nevada. *Geology* 27:215-218.

GLUMAC, B., and WALKER, K.R., 1998. A Late Cambrian positive carbon-isotope excursion in the southern Appalachians: relation to biostratigraphy, sequence stratigraphy, environments of deposition, and diagenesis. *Journal of Sedimentary Research*, 68:1212-1222.

GOODMAN, W.M., and BRETT, C.E., 1994. Roles of eustasy and tectonics in development of Silurian stratigraphic architecture of the Appalachian foreland basin. In: Dennison, J.M., and Ettensohn, F.R., Eds., *Tectonic and eustatic controls on sedimentary cycles*, 147-169. Society of Economic and Petroleum Mineralogists, Concepts in sedimentology and paleontology, 4.

HALFAR, J., GODINEZ-ORTA, L., MUTTI, M., VALDEZ-HOLGUÍN, J.E., and BORGES, J.M., 2004. Nutrient and temperature controls on modern carbonate production: an example from the Gulf of California, Mexico. *Geology*, 32:213-216.

HALL, J.A., 1839. Third annual report of the Fourth Geological District of New York. *New York State Geological Survey annual report*, 3:287-374.

HALLOCK, P., 1988. The role of nutrient availability in bioerosion: consequences to carbonate buildups. *Palaeogeography, Palaeoclimatology, Palaeoecology*, 63:275-291.

———, 2001. Coral reefs, carbonate sediments, nutrients, and global change. In Stanley, G.D., Ed., *The history and sedimentology of ancient reef systems*, 387-427. New York: Kluwer Academic and Plenum Publishers.

HERBERT, T.D., and SARMIENTO, J.L., 1991. Ocean nutrient distribution and oxygenation: Limits on the formation of warm saline bottom water over the past 91 m.y. *Geology*, 19: 702-705.

HORVATH, A.L., 1969. Relationships of middle Silurian strata in Ohio and West Virginia. *The Ohio Journal of Science*, 69:321-342.

JEPPSSON, L., 1983. Silurian conodont faunas from Gotland. *Fossils and Strata*, 15:121-144.

———, 1987. Lithological and conodont distributional evidence for episodes of anomalous oceanic conditions during the Silurian. In: Aldridge, R.J., Ed., *Palaeobiology of conodonts*: 129-145. Chichester, Ellis Horwood Ltd.

———, 1990. An oceanic model for lithological and faunal changes tested on the Silurian record. *Journal of the Geological Society of London*, 147:663-674.

———, 1997a. A new latest Telychian, Sheinwoodian, and Early Homerian (Early Silurian) Standard Conodont Zonation. *Transactions of the Royal Society of Edinburgh, Earth Sciences*, 88:91-114.

———, 1997b. The anatomy of the Mid-Early Silurian Ireviken event and a scenario for P-S events. In: Brett, C.E., and Baird, G.C., Eds., *Paleontological events: stratigraphic, ecological and evolutionary implications*, 451-492. New York: Columbia University Press.

———, 1998. Silurian oceanic events: summary of general characteristics. In: Landing, E., and Johnson, M.E., Eds., Silurian cycles: Linkages of dynamic stratigraphy with atmospheric, oceanic and tectonic changes. *New York State Museum Bulletin*, 491:239-257.

JEPPSSON, L., ALDRIDGE, R.J., and DORNING K.J., 1995. Wenlock (Silurian) oceanic episodes and events. *Journal of the Geological Society of London*, 152:487-498.

JOACHIMSKI, M.M., and BUGGISCH, W., 1993. Anoxic events in the late Frasnian – causes of the Frasnian-Fammenian faunal crisis? *Geology*, 21:675-678.

JOHNSON, M.E., RONG, J., WANG, C., and WANG, P., 2001. Continental island from the Upper Silurian (Ludfordian Stage) of Inner Mongolia: implications for eustasy and paleogeography. *Geology*, 29:955-958.

KALJO, D., KIIPLI, T., and MARTMA, T., 1997. Carbon isotope event markers through the Wenlock-Pridoli sequence at Ohesaare (Estonia) and Priekule (Latvia). *Palaeogeography, Palaeoclimatology, Palaeoecology*, 132:211-233.

KLEFFNER, M.A., 1991. Conodont biostratigraphy of the upper part of the Clinton Group and the Lockport Group (Silurian) in the Niagara Gorge region, New York and Ontario. *Journal of Paleontology*, 65:500-511.

KLUESSENDORF, J., and MIKULIC, D.G., 1996. An early Silurian sequence boundary in Illinois and Wisconsin. In: Witzke, B.J., Ludvigson, G.A., and Day, J., Eds., *Paleozoic sequence stratigraphy: views from the North American craton*, 177-185. Geological Society of America Special Paper 306.

KUMP, L.R., and ARTHUR, M.A., 1999. Interpreting carbon-isotope excursions: carbonates and organic matter. *Chemical Geology*, 161:181-198.

KUMP, L.R., ARTHUR, M.A., PATZKOWSKY, M.E., GIBBS, M.T., PINKUS, D.S., and SHEEHAN, P.M., 1999. A weathering hypothesis for glaciation at high atmospheric pCO2 during the late Ordovician. *Palaeogeography, Palaeoclimatology, Palaeoecology*, 152:173-187.

LÜNING, S., LOYDELL, D.K., SUTCLIFFE, O., AIT SALEM, A., ZANELLA, E., CRAIG, J., and HARPER, D.A.T., 2000a. Silurian-Lower Devonian black shales in Morocco: which are the organically richest horizons? *Journal of Petroleum Geology*, 23:293-311.

LÜNING, S., CRAIG, J., LOYDELL, D.K., STORCH, P., and FITCHES, B., 2000b. Lower Silurian "hot" shales in North Africa and Arabia: regional distribution and depositional model. *Earth Science Reviews*, 49:121-200.

MABILLARD J.E., and ALDRIDGE, R.J., 1985. Microfossil distribution across the base of the Wenlock series in the type area. *Palaeontology*, 28:89-100.

MAGARITZ, M., 1983. Carbon and oxygen isotope composition of recent and ancient coated grains. In: Peryt, T.M., Ed. *Coated Grains*, 27-37. Berlin, Springer.

MELCHIN, M.J., 1994. Graptolite extinction at the Llandovery-Wenlock boundary. *Lethaia*, 27:285-290.

MELCHIN, M.J., RONG, J.-Y., GRADSTEIN, F., KOREN, T.N., and FINNEY, S.C., 2004. Stability in stratigraphy. *Lethaia*, 37:124-125.

MII, H., GROSSMAN, E.L., and YANCEY, T.E., 1999. Carboniferous isotope stratigraphies of North America: implications for Carboniferous paleoceanography and Mississippian glaciation. *Geological Society of America Bulletin*, 111:960-973.

MIKULIC, D.G., and KLUESSENDORF, J., 1999. Stasis and extinction of Silurian (Llandovery-Wenlock) trilobite associations related to oceanic cyclicity. *Journal of Paleontology*, 73:320-325.

MOORE, G.T., HAYASHIDA, D.N., and ROSS, C.A., 1993. Late early Silurian (Wenlockian) general circulation model-generated upwelling, graptolitic black shales, and organic-rich source rocks – an accident of plate tectonics? *Geology*, 21:17-20.

MUNNECKE, A., WESTPHAL, H., REIJMER, J.J.G., and SAMTLEBEN, C., 1997. Microspar development during early marine burial diagenesis: a comparison of Pliocence carbonates from the Bahamas with Silurian limestones from Gotland (Sweden). *Sedimentology*, 44:977-990.

MUNNECKE, A., SAMTLEBEN, C., and BICKERT, T., 2003. The Ireviken Event in the lower Silurian of Gotland, Sweden – relation to similar Palaeozoic and Proterozoic events. *Palaeogeography, Palaeoclimatology, Palaeoecology*, 195:99-124.

MURPHY, M.A., DUNHAM, J.B., BERRY, W.B.N., and MATTI, J.C., 1979. Late Llandovery unconformity in central Nevada. *Brigham Young University Geology Studies*, 26:21-36.

O'BRIEN, N.R., BRETT, C.E., and WOODARD, M.J., 1998. Shale fabric as a clue to sedimentary processes – example from the Williamson-Willowvale Shales (Silurian), New York. In: Shieber, J., Zimmerle, W., and Sethi, P.S., Eds., *Shales and Mudstones II*, 55-66. Stuttgart, Springer-Verlag.

PARRISH, J.T., 1982. Upwelling and petroleum source beds, with reference to the Paleozoic. *American Association of Petroleum Geologists Bulletin*, 66:750-774.

PARRISH, J.T., ZIEGLER, A.M., and HUMPHREVILLE, R.G., 1983. Upwelling in the Paleozoic Era. In: Seuss, E., and Thiede, J., Eds., *Coastal upwelling, its sediments record; part b, sedimentary records of ancient coastal upwelling*, 553-578. New York: Plenum Press.

PATTERSON, W.P., and WALTER, L.M., 1994. Depletion of 13C in seawater ÓCO2 on modern carbonate platforms: significance for the carbon isotopic record of carbonates. *Geology*, 22:885-888.

POPE, M.C., and STEFFEN, J.B., 2003. Widespread, prolonged late Middle to Late Ordovician upwelling in North America: a proxy record of glaciation?. *Geology*, 31:63-66.

RANKEY, E.C., 2004. On the interpretation of shallow shelf carbonate facies and habitats: how much does water depth matter? *Journal of Sedimentary Research*, 74:2-6.

RIPPERDAN, R.L., MAGARITZ, M., NICOLL, R.S., and SHERGOLD, J.H., 1992. Simultaneous changes in carbon isotopes, sea-level and conodont biozones within the Cambrian-Ordovician boundary interval at Black Mountain, Australia. *Geology, 20:1039-1042.*

SALTZMAN, M.R., 2001. Silurian $\delta^{13}C$ stratigraphy: a view from North America. *Geology*, 29:671-674.

———, 2002a. Carbon isotope $\delta^{13}C$ stratigraphy across the Silurian-Devonian transition in North America: evidence for a perturbation of the global carbon cycle. *Palaeogeography, Palaeoclimatology, Palaeoecology*, 187:83-100.

———, 2002b. Carbon and oxygen isotope stratigraphy of the Lower Mississippian (Kinderhookian – early Osagean), western United States: implications for seawater chemistry and glaciation. *Geological Society of America Bulletin*, 114:96-108.

———, 2005. Phosphorus, nitrogen, and the redox evolution of the Paleozoic oceans. *Geology*, 33:573-576.

SALTZMAN, M.R., and YOUNG, S.A., 2005. Long-lived glaciation in the Late Ordovician? isotopic and sequence stratigraphic evidence from western Laurentia. *Geology* , 33:109-112.

SALTZMAN, M.R., RUNNEGAR, B., and LOHMANN, K.C., 1998. Carbon isotope stratigraphy of upper Cambrian (Steptoean Stage) sequences of the eastern Great Basin: Record of a global oceanographic event. *Geological Society of America Bulletin*, 110:285-297.

SALTZMAN, M.R., RIPPERDAN, R.L., BRASIER, M.D., LOHMANN, K.C., ROBISON, R.A., CHANG, W.T., PENG, S., ERGALIEV, E.K., and RUNNEGAR, B., 2000. A global carbon isotope excursion (SPICE) during the late Cambrian: Relation to trilobite extinctions, organic matter burial and sea level. *Palaeogeography, Palaeoclimatology, Palaeoecology*, 162:211-223.

SAMTLEBEN, C., MUNNECKE, A., BICKERT, T., and PÄTZOLD, J., 1996. The Silurian of Gotland (Sweden): Facies interpretation based on stable isotopes in brachiopod shells. *Geologische Rundschau*, 85: 278-292.

SHAVER, R.H., 1996. Silurian sequence stratigraphy in the North American craton, Great Lakes area. In: Witzke, B.J., Ludvigson, G.A., and Day, J., Eds. Paleozoic sequence stratigraphy: views from the North American craton. *Geological Society of America Special Paper*, 306:193-202.

SMETHURST, M.A., and MCENROE, S.A., 2003. The palaeolatitude controversy in the Silurian of Newfoundland resolved: new palaeomagnetic results from the central mobile belt. *Tectonophysics*, 362:83-104.

VAN DER VOO, R., 1988. Paleozoic paleogeography of North America, Gondwana, and intervening displaced terranes: comparisons of paleomagnetism with paleoclimatology and biogeographical patterns. *Geological Society of America Bulletin*, 100:311-324.

WANG, K., GELDSETZER, H.H.J., GOODFELLOW, W.D., and KROUSE, H.R., 1996. Carbon and sulfur isotope anomalies across the Frasnian-Famennian extinction boundary, Alberta, Canada. *Geology*, 24:187-191.

WITZKE, B.J., 1987. Models for circulation patterns in epicontinental seas applied to Paleozoic facies of North American craton. *Paleoceanography*, 2:229-248.

WITZKE, B.J., and SCOTESE, C.R., 1990. Palaeoclimatic constraints for Palaeozoic palaeolatitudes of Laurentia and Euramerica. In: Scotese, C.R., Ed., *Geological Society of London Memoir*, 12:57-73.

WOODCOCK, N.H., 2000. Introduction to the Silurian. *Geologic Conservation Review Series*, 19:3-22.

Manuscript received May 3, 2005
Manuscript accepted October 6, 2005